DIURNAL, SEASONAL AND SOLAR CYCLE VARIATION OF TOTAL ELECTRON CONTENT AND COMPARISON WITH IRI-2016 MODEL AT BIRNIN-KEBBI

Aghogho Ogwala,[1,*]Emmanuel Olufemi Somoye,[1]Olugbenga Ogunmodimu.,[3]Rasaq Adewemimo Adeniji-Adele,[1]Eugene Oghenakpobo Onori,[1]Oluwole Oyedokun[2]

[1,*] Department of Physics, Lagos State University, Lagos, Nigeria.

[2] Department of Physics, University of Lagos, Nigeria.

[3] Department of Electrical Engineering, Manchester Metropolitan University, United Kingdom.

ABSTRACT

Total Electron Content (TEC) is an important ionospheric parameter used to monitor possible space weather impacts on satellite to ground communication and satellite navigation system. TEC is modified in the ionosphere by changing solar Extreme Ultra-Violet (EUV) radiation, geomagnetic storms, and the atmospheric waves that propagate up from the lower atmosphere. Therefore, TEC depends on local time, latitude, longitude, season, geomagnetic conditions, solar cycle activity, and condition of the troposphere. A dual frequency GPS receiver located at an equatorial station, Birnin-Kebbi in Northern Nigeria (geographic location: 12.64°N; 4.22°E; 2.68°N dip), has been used to investigate variation of TEC during the period of 2011 to 2014. We investigate the diurnal, seasonal and solar cycle dependence of observed (OBS) TEC and comparison with latest version of International Reference Ionosphere (IRI-2016) model. On a general note, diurnal variation reveals discrepancies between OBS-TEC and IRI-2016 model for all hours of the day except during the post-midnight hours. Slight post-noon peaks in the daytime maximum and post-sunset decrease and enhancement are observed in the diurnal variation of OBS-TEC of some months. On a seasonal scale, we observed that OBS-TEC values were higher in the

equinoxes than the solstices only in 2012. Where as in 2011, September equinox and December solstice recorded higher magnitude followed by March equinox and lowest in June solstice. In 2013, December solstice magnitude was highest, followed by the equinoxes and lowest in June solstice. In 2014, March equinox and December solstice magnitude were higher than September equinox and June solstice magnitude. June solstice consistently recorded the lowest values for all the years. OBS-TEC is found to increase from 2011 to 2014, thus revealing solar cycle dependence.

KEYWORDS: TEC; diurnal; seasonal; variation; solar cycle 24; IRI-2016.

CORRESPONDING AUTHOR PHONE: +234 8055650264

CORRESPONDING AUTHOR E-MAIL:ogwala02@gmail.com

INTRODUCTION

48 The ionosphere causes a variation in the intensity of radio signals – fading – as a result of
49 irregularities (inhomogeneity in electron density) (Somoye, 2010; Ogwala *et al.* 2018,
50 Ogunmodimu *et al.* 2018). Akala *et al.,* (2011) reported that the variable nature of the equatorial/
51 low latitude ionosphere threatens communication and navigation/ satellite systems. The equatorial/
52 low latitude ionosphere exhibits many unique features such as the seasonal anomaly, semi-annual
53 anomaly, equinoctial anomaly, noon bite-out, spread-F, equatorial electrojet (EEJ), equatorial
54 plasma bubbles (EPB) (Stankov, 2009; Maruyama *et al.*, 2004; Jee *et al.,* 2004; Codrescu *et al.*,
55 1999).

56 For many decades, scientists have been studying these ionospheric features and the role
57 they play in trans-ionospheric electromagnetic radio wave propagation. These studies are carried
58 out using different techniques and instruments. One of the instruments used is the GPS receiver,
59 which provide direct measurements from satellites. Their sounding capacity extends to the topside
60 of the ionosphere, but is affected by time and space constraints (Ciraolo and Spalla, 2002).
61 Recently, GPS receiver is the most efficient method used to eliminate the effect of the ionosphere
62 on radio signals. This method combines signals in different L band frequencies, L1 (1575 MHz)
63 and L2 (1228 MHz).

64 Almost all space geodetic techniques transmit signals in at least two different frequencies
65 for better accuracy (Alizadeh *et al.,* 2013). These are combined linearly and can greatly eliminate
66 the effect of the ionosphere on radio signals. The ionospheric effect on radio signal is proportional
67 to total electron content (TEC), which is defined as the number of electrons per square meter from
68 satellite in space to receiver on ground is shown in equation (1).

69 $$TEC = \int n_e(s)ds \qquad (1)$$

It is measured in multiples of TEC units (1 TECU = 10^{16} el/m^2). Due to the dispersive nature of the ionosphere, there is a time delay between the two frequencies of a GNSS signal as it propagates through the ionosphere as shown in Equation (2) as $\Delta t = t_2 - t_1$. Thus,

$$\Delta t = \left(\frac{40.3}{C}\right) \times \frac{TEC}{\left[\left({}^{1}/_{f_2^2}\right) - \left({}^{1}/_{f_1^2}\right)\right]} \quad (2)$$

Where c is speed of light and f is frequency. Hence, Δt measured between the L1 and L2 frequencies is used to evaluate TEC along the ray path.

When Global Navigation Satellite System (GNSS) signals propagate through the ionosphere, the carrier experiences phase advance and the code experiences a group delay due to the electron density along the line of sight (LOS) from the satellite to the receiver (Bagiya *et al.,* 2009; Tariku, 2015). Thus, the carrier phase pseudo ranges are measured too short, and the code pseudo ranges are measured too long compared to the geometric range between the satellite and the receiver. This results in a range error of the positioning accuracy provided by a GPS receiver. The range error due to TEC in the ionosphere varies from hundreds of meters at mid-day, during high solar activity when the satellite is near the horizon of the observer, to a few meters at night during low solar activity, with the satellite positioned at zenith angle (Bagiya *et al.,* 2009). By measuring this delay using dual frequency GPS receivers, properties of the ionosphere can be inferred and used to monitor space weather events such as GNSS, HF communications, Space Based Observation Radar and Situational Awareness Radar, etc. It is documented that ionospheric delay which is proportional to TEC is the highest contributor to GPS positioning error (Alizadeh *et al.,* 2013; Akala *et al.,* 2013).

TEC in the ionosphere can also be studied using empirical ionospheric model such as the International Reference Ionosphere (IRI). IRI is a joint undertaking by the Committee on Space

92 Research (COSPAR) and International Union of Radio Science (URSI) with the goal of developing
93 and improving an international standard for the parameters in earth's ionosphere (Bilitza *et al.*,
94 2014). An updated version has been developed recently to cater for lapses of previous models. IRI
95 provides the vertical TEC (VTEC) from the lower boundary (60 – 80 km) to a user-specific upper
96 boundary (Bilitza *et al.*, 2016).

97 In the past few decades, studies on the temporal and spatial variations of TEC have gained
98 popularity in the scientific community (Wu *et al.*, 2008). However, understanding the variability
99 of TEC will also go a long way in obtaining the positioning accuracy of GNSS under disturbed
100 and quiet conditions. The global distribution of TEC variations and its characteristics at all
101 latitudes, during different solar cycle phases under disturbed and quiet conditions have been
102 investigated by some researchers (Bhuyan and Borah, 2007; Maruyama *et al.*, 2004; Jee *et al.*,
103 2004).

104 Rama Rao *et al.* (2006a, b); Wanninger (1993) reported maximum day-to-day variability
105 in TEC at the Equatorial Ionization Anomaly (EIA) crest regions, increasing peak value of TEC
106 with increase in integrated equatorial electrojet (IEEJ) strength, maximum monthly average
107 diurnal variations during equinox months followed by winter months and lowest during summer
108 months. They also reported positive correlation of TEC and EEJ and the spatial variation of TEC
109 in the equatorial region. Titheridge (1974) and Langley *et al.* (2002) attributed the lower TEC
110 values during the summer seasons to low ionization density resulting from reduced O/ N_2 ratio
111 (production rates) which is a result of increased scale height. Bhuyan and Borah (2007); Komjathy
112 *et al.* (1998); Lee and Reinisch (2006) compared TEC derived from GPS receivers with IRI model
113 in the equatorial/ low latitude sector and inferred that the diurnal amplitude of TEC is higher during
114 the equinoxes followed by December solstices and lowest in June solstice, i.e., observing winter

anomaly in seasonal variation. Malik *et al*. (2016) reported higher IRI values than observed maximum useable frequency (MUF) values but behaves similarly diurnally and seasonally with no clear trend. Akala *et al*. (2013) on the comparison of equatorial GPS-TEC observations over an African station and an American station during the minimum and ascending phases of solar cycle 24 reported that seasonal VTEC values were maximum and minimum during March equinox and June solstice respectively, during minimum solar cycle phase at both stations. They also reported that during the ascending phase of solar cycle 24, minimum and maximum seasonal VTEC values were recorded during December solstice and June solstice respectively. They further showed that IRI-2007 model predicted better in the American sector than the African sector.

In this research, the result obtained in 2012 and 2013 which corresponds to the result of these researchers. However, the result we obtained in 2011 and 2014 did not follow the trend reported by these researchers, who explored the equatorial/ low latitude during different solar cycle epochs. We also observed discrepancies between the OBS-TEC and IRI-2016 almost throughout the day for all the years in this research.

DATA AND METHODOLOGY

2.1 DATA

The Receiver Independence Exchange (RINEX) Observation GPS data files were downloaded daily from NIGNET website (www.nignet.net) and processed using Bernese software and GPS TEC analysis software. The RINEX file contains 60 iteration data (i.e. in 1 minute time resolution). The GPS-TEC analysis software was designed by Gopi Seemala of the Indian Institute of Geomagnetism. The summary of this application are, reads raw data, processes cycle slips in phase data, reads satellite biases from the International GNSS services (IGS) code files (and

calculates them if unavailable), and calculates receiver bias, inter-channel biases for different satellites in the constellation, and finally plots the VTEC values on the screen and writes the ASCII output files (*CMN) for STEC and (*STD) for VTEC in the same directory of the data files. Effect due to multipath is eliminated by using a minimum elevation angle of 50°.

Observation GPS-TEC obtained from the TEC analysis software is the slant TEC (STEC) and vertical TEC (VTEC). STEC is polluted with several biases that must be eliminated to get VTEC. VTEC is calculated from the daily values of STEC using equation (3).

$$VTEC = (STEC - [b_R + b_S + b_{RX}])/S(E) \quad (3)$$

Where b_R, b_S, and b_{RX} are receiver bias, satellite bias receiver interchannel bias respectively. S(E), which is the oblique factor with zenith angle, z at IPP (Ionospheric Pierce Point) is expressed in equation (4).

$$S(E) = \frac{1}{\cos(z)} = \left\{1 - \left(\frac{R_E \times \cos(E)}{R_E + h_S}\right)^2\right\}^{-0.5} \quad \text{Bolaji } \textit{et al.} \text{ (2012)} \quad (4)$$

R_E = the mean radius of the earth in km and h_S = ionospheric height from the surface of the earth. According to Rama Rao *et al.*, (2006c), ionospheric shell height of approximately 350km is appropriate for the equatorial/ low latitude region of the ionosphere for elevation cut off angle of > 50°. This is valid in this study.

Hourly VTEC data obtained from these processing software are averaged to daily TEC values in TEC units (1 TECU = 10^{16} el/m^2). OBS-TEC from Birnin-kebbi, on geographic Latitude 12.47°N and geographic Longitude 4.23°E located in Northern Nigeria, obtained during the period 2011 – 2014, which corresponds to the ascending (2011 – 2013) and maximum (2014) phases of solar cycle 24 were compared with derived TEC obtained from International Reference Ionosphere (IRI-2016) model website (https://ccmc.gsfc.nasa.gov/modelweb/models/iri2016_vitmo.php). The 2016 version of IRI provides important changes and improvements on previous IRI versions

(Bilitza *et al.*, 2016). Solar cycle 24 is regarded as a quiet solar cycle which peaked in 2014 with maximum sunspot number (103) occurring in February. Values of sunspot number, Rz, in Text format were obtained from Space Physics Interactive Data Resource (SPIDR) website (www.ionosonde.spidr.com) before it became unavailable. Table 1 shows the years used in this study and their corresponding sunspot number, Rz.

Table I: Table of years, solar cycle phase and sunspot number, Rz [Source: Author].

Years	**Solar Cycle Phase**	**Sunspot Number, R_z**
2011	Ascending	55.7
2012	Ascending	57.6
2013	Ascending	64.7
2014	Maximum	79.6

2.2 METHODOLOGY

Comparison of diurnal variations of hourly OBS-TEC with error bars and hourly IRI-2016 model (NeQuick topside option) were plotted using the monthly mean values of OBS-TEC and monthly mean of IRI-2016 model with respect to local time (LT). The corresponding percentage deviation (percentage Dev or % DEV) of IRI-2016 from OBS-TEC were also analysed using using the monthly mean values of OBS-TEC monthly mean values of IRI-2016 with respect to local time (LT). Percentage Dev is obtained using equations (5) below:

$$\%DEV = \left(\frac{OBS-IRI}{OBS}\right) \times 100 \quad (5)$$

where OBS represents Observation-TEC values and IRI represents TEC derived by IRI-2016.

The OBS-TEC data was grouped following Onwumechilli and Ogbuehi (1964) into four seasons namely: March equinox (February, March and April), June solstice (May, June and July), September equinox (August, September and October) and December solstice (November, December and January), in order to investigate seasonal variation. Finally, Annual variation of OBS-TEC and sunspot number, Rz were also analysed by plotting mean OBS-TEC and mean Rz against each month of the year.

RESULT AND DISCUSSIONS

Figures 1 to 4 shows the diurnal variation of OBS-TEC and IRI-2016 model in the Nigerian Equatorial Ionosphere (NEI) for the years 2011 to 2014 respectively. OBS-TEC were obtained from the GPS receiver installed at Birnin-Kebbi station. The diurnal variation of OBS-TEC and IRI-2016 model TEC reveals the typical characteristics of an equatorial/ low latitude ionosphere. Generally, the day-to-day variation of OBS-TEC have been indicated using the top and bottom error bar. The study reveals that day-to-day variation of OBS-TEC is higher during the daytime than night time for all the years. It well known fact that during the day, the sun causes variations in temperature, neutral wind, electron density and electric field thereby modulating the structure and evolution of the ionosphere and thermosphere (Gorney, 1990; Forbes *et al.* (2006). These Figures shows a steep rise in OBS-TEC from a minimum of ~2 TECU between 03:00 – 05:00 LT in 2011, ~3 TECU (04:00 – 05 LT) in 2012, ~3 TECU (03:00 – 05:00 LT) in 2013 and 2014. OBS-TEC increased to a broad daytime maximum between 00:12 LT – 00:14 LT for all years before falling to a minimum after sunset. The diurnal variation of IRI-2016 model shows TEC increasing from a minimum of ~ 2 TECU in 2011, ~ 4 TECU in 2012 and 2013, and ~ 5 TECU in 2014 between 03:00 – 04:00 LT for all years, to a broad daytime peak between 08:00 – 14:00 LT, before falling steeply to minimum before sunset. Hence the IRI-2016 model attained its peak before OBS-

TEC. Dabas *et al.* (2003); Somoye *et al. (*2011); Hajra *et al.* (2016); D'ujanga *et al.* (2017) attributed the steep increase in TEC to solar EUV ionization and upward vertical E × B resulting from the rapid filling up of the magnetic field tube at sunrise and meridional winds (Suranya *et al.*, 2015). These magnetic field tubes collapse after sunset due to low thermospheric temperature and Releigh Taylor Instability (RTI) (Ayorinde *et al.*, 2016) giving rise to the minimum TEC values after sunset. These results are similar to findings of Bolaji *et al.*, (2012), Fayose *et al.*, (2012), Okoh *et al.*, (2014), Eyelade *et al.*, (2017) who have explored the NEI.

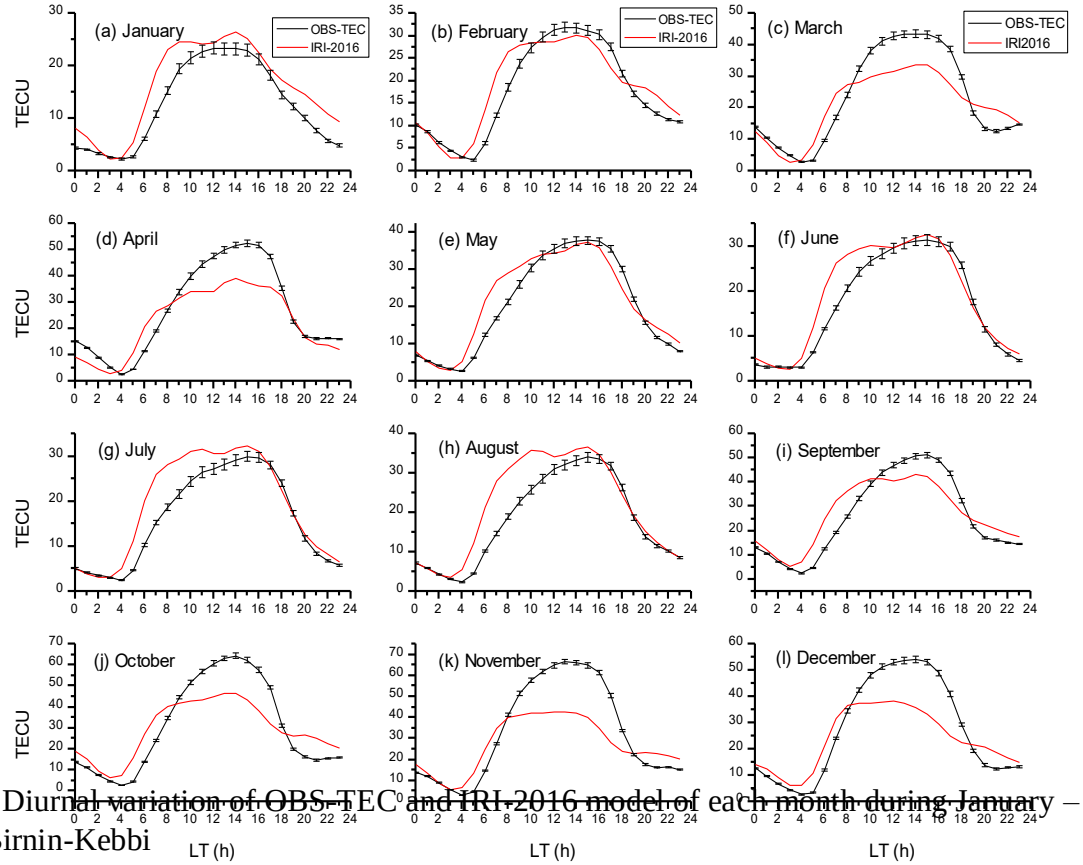

Figure 1: Diurnal variation of OBS-TEC and IRI-2016 model of each month during January – December 2011 at Birnin-Kebbi

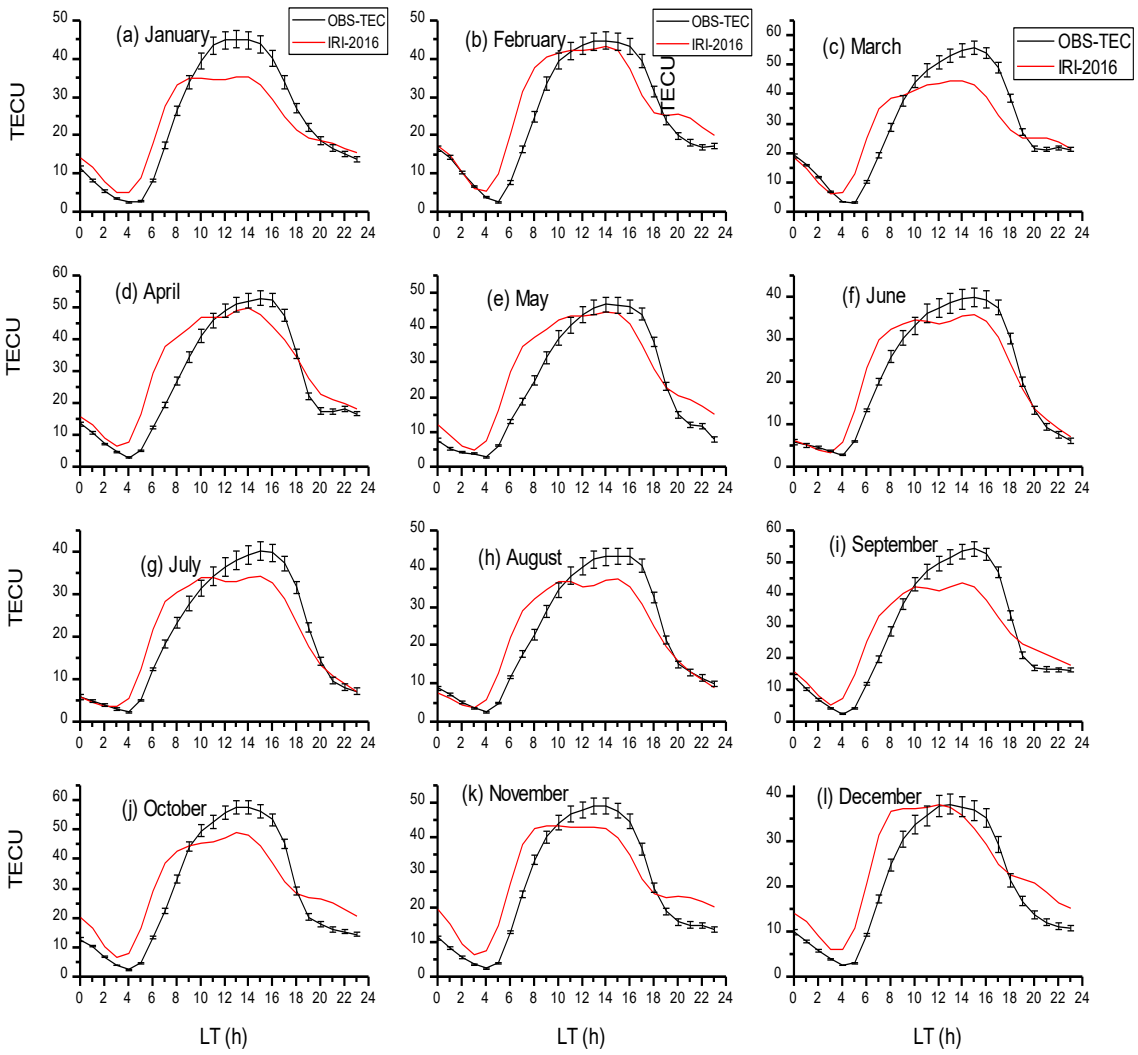

Figure 2: Diurnal variation of OBS-TEC and IRI-2016 model of each month during January – December 2012 at Birnin-Kebbi

220

221

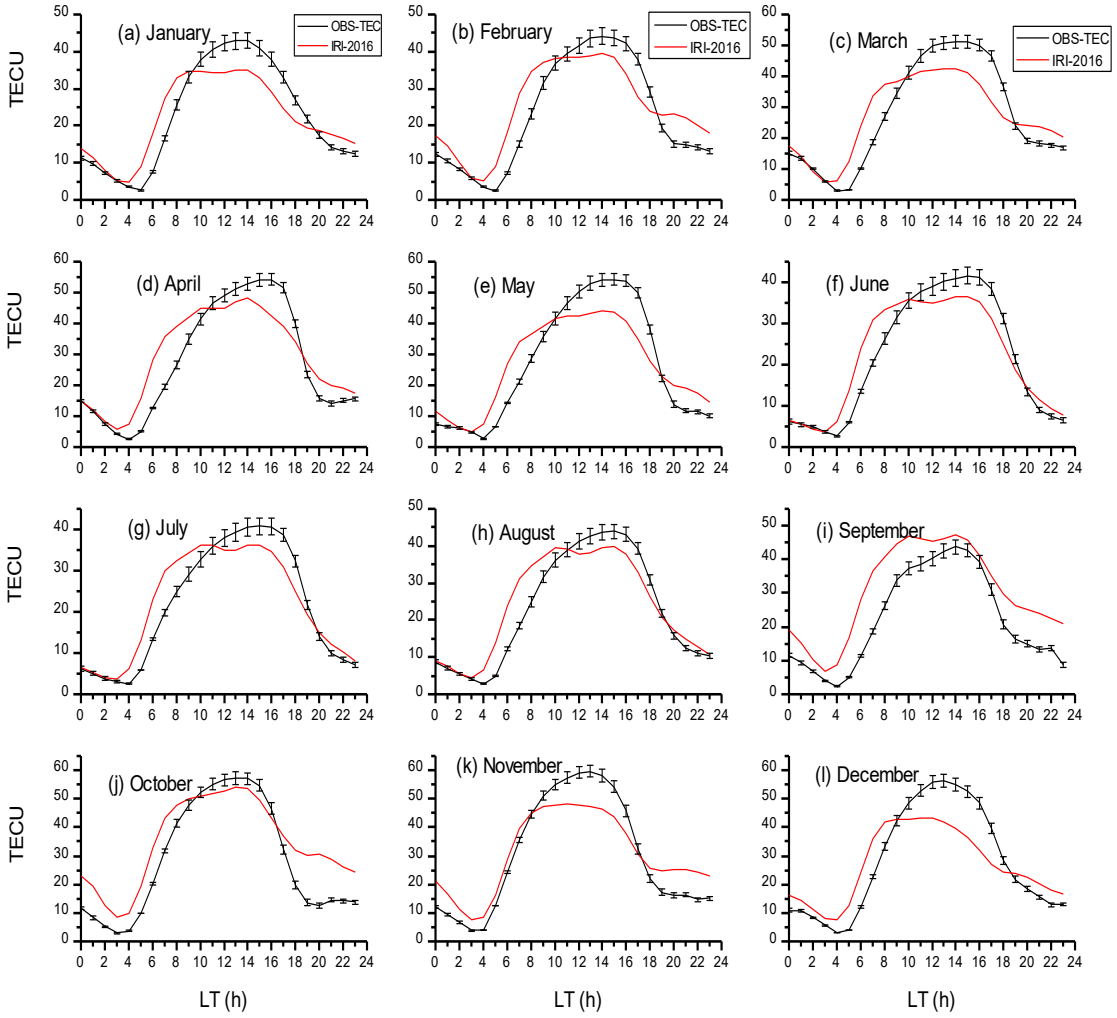

Figure 3: Diurnal variation of OBS-TEC and IRI-2016 model of each month during January – December 2013 at Birnin-Kebbi

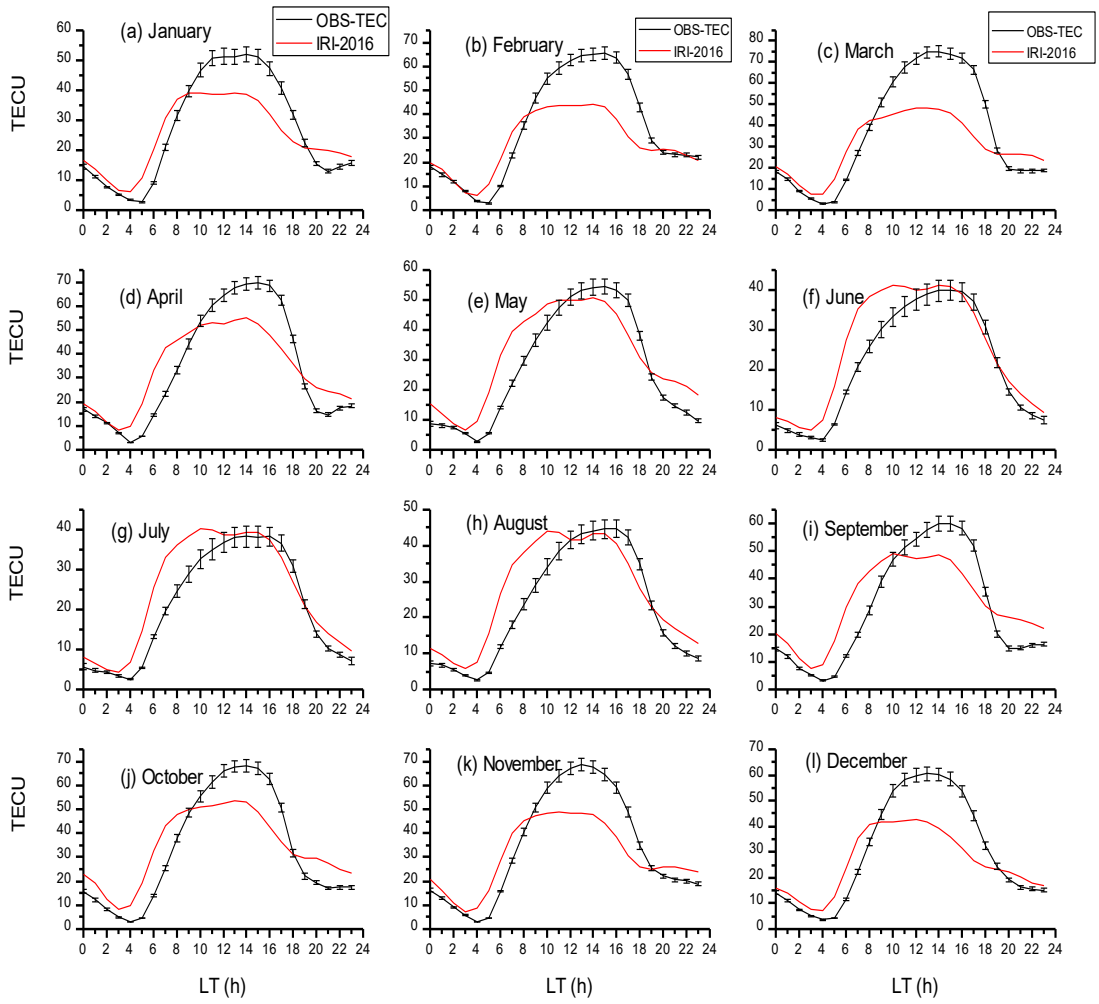

Figure 4: Diurnal variation of OBS-TEC and IRI-2016 of each month during January – December 2014 at Birnin-Kebbi

It can be seen that OBS-TEC is much higher in 2014 with maximum values up to 70 TECU in March compared with IRI-2016 maximum of 54 TECU in the month of October, 2014. The diurnal variation reveals that the peak of OBS-TEC of some months was delayed till after noon. For example, the months of April, July, August and September in 2011, March, April, June and September in 2012, April, June, July and September in 2013 had delayed peak. The delayed OBS-TEC peaks were also seen in April, May, June, August and September of 2014. This type of peak

shifting is peculiar to the Polar Regions and it is found to depend on the solar zenith angle. Another major phenomenon seen in the diurnal variation of OBS-TEC is the post-sunset decrease and slight enhancement in some months. The night time enhancement of TEC, for example, March, April and October of the year 2011, March and April of the year 2012, March, April, September and October of the year 2013, January, April and September of the year 2014 was documented by previous researchers like Rama Rao *et al.,* 2009; D'ujanga *et al.,* 2017. They attributed it to the product of eastward and westward directed electric field which produces an upward and downward motion of ionospheric plasma during the day and night respectively.

Figures 5 to 8 shows the diurnal variation of percentage deviation of IRI-2016 model from OBS-TEC in the Nigerian Equatorial Ionosphere (NEI) for all years respectively. On a general note, IRI-2016 model only presented suitable predictions for the post-midnight hour between 00 – 05hr of the day for all years. All other hours from 06 – 23hr shows some discrepancies. In some months, these discrepancies lasted throughout the day for example, in the months of October, November and December of 2012, October and December, 2013, and September and October of 2014, while in some other months these discrepancies collapsed during the pre-midnight hours, for example, in the months of June, July and August of 2011, June, July and August of 2012, June and August of 2013 and February, June and July of 2014. It is also important to mention that IRI-2016 model either over estimated or under estimated TEC in the NEI especially during daytime hours as shown in plots.

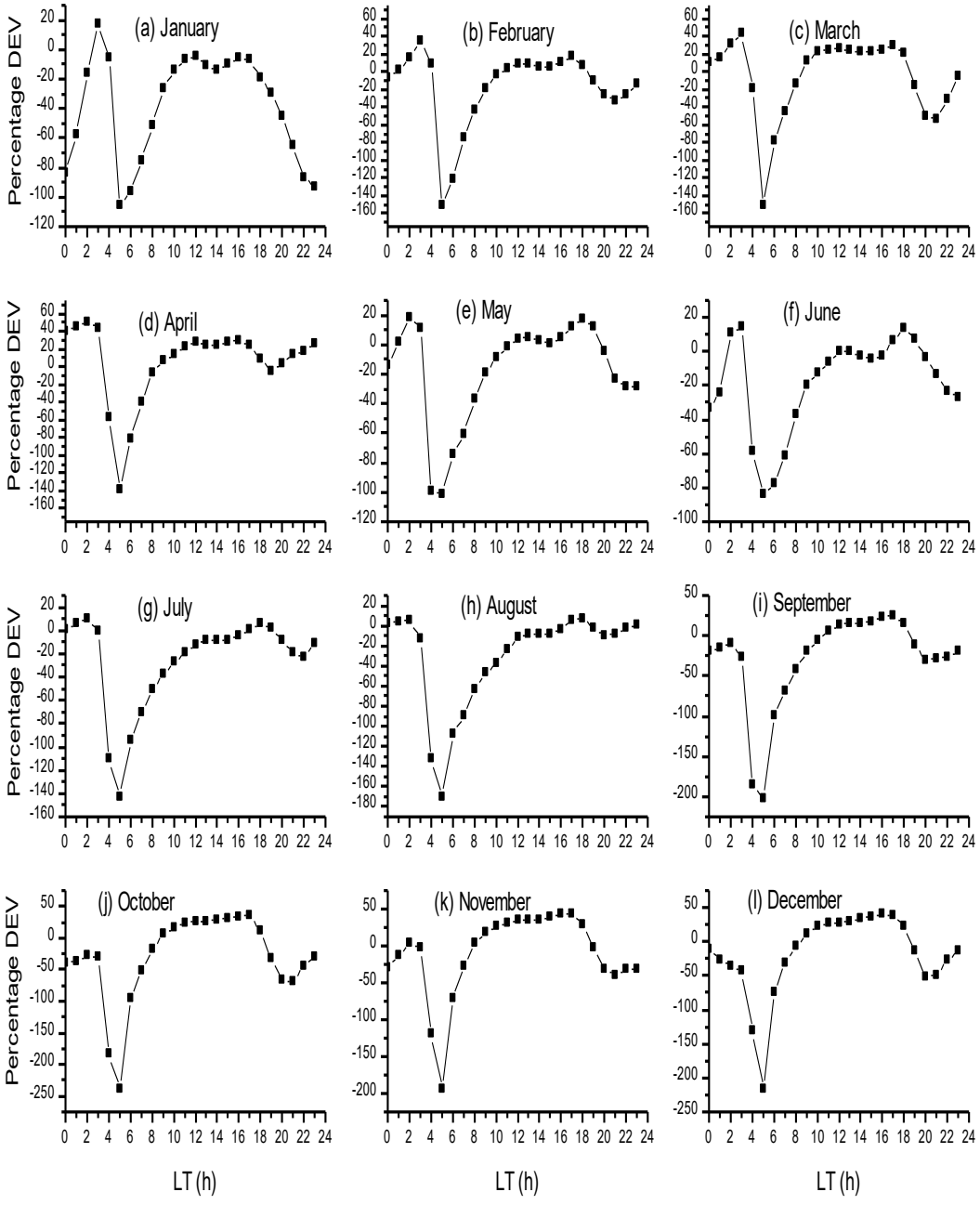

Figure 5: Percentage deviation of IRI-2016 from OBS-TEC for year 2011

257

258

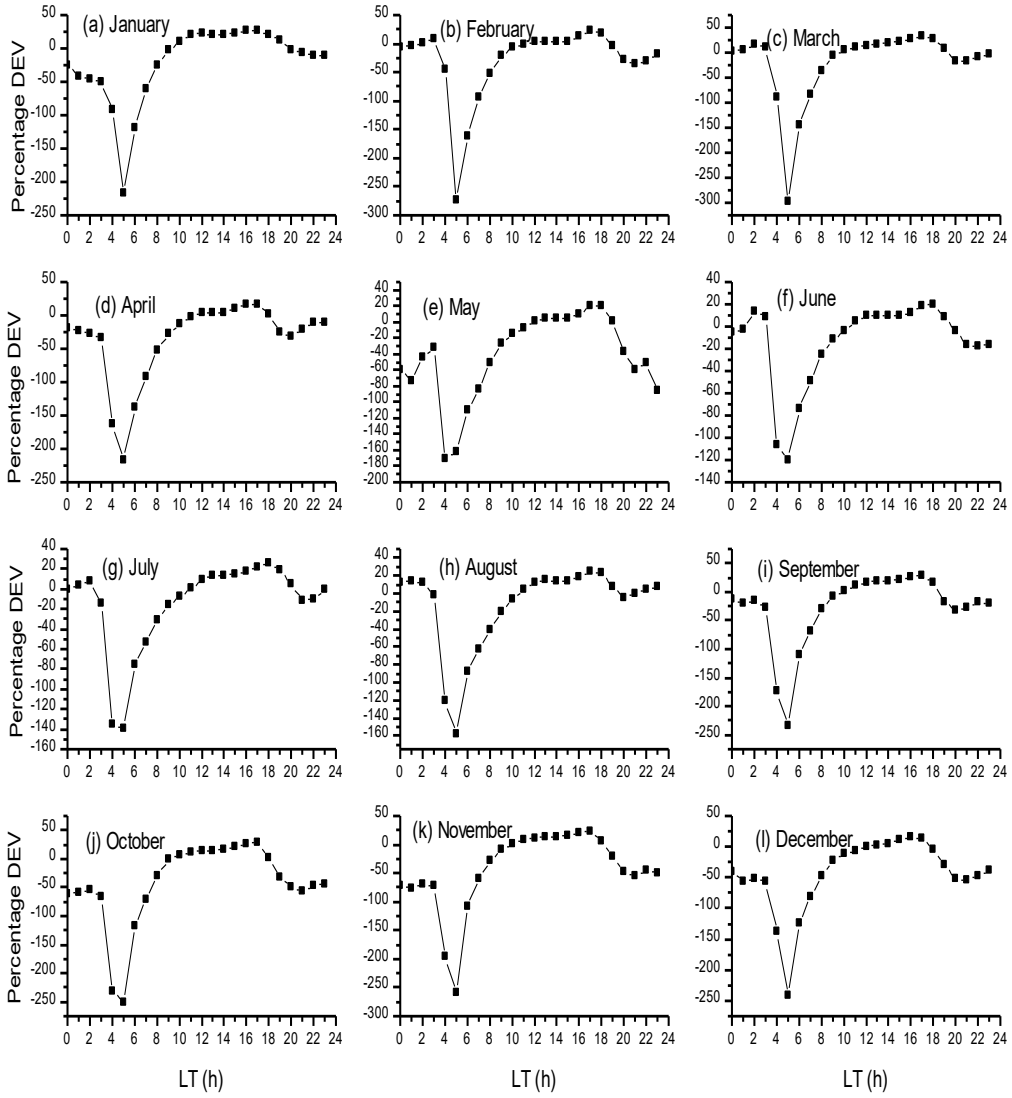

Figure 6: Percentage deviation of IRI-2016 from OBS-TEC for year 2012

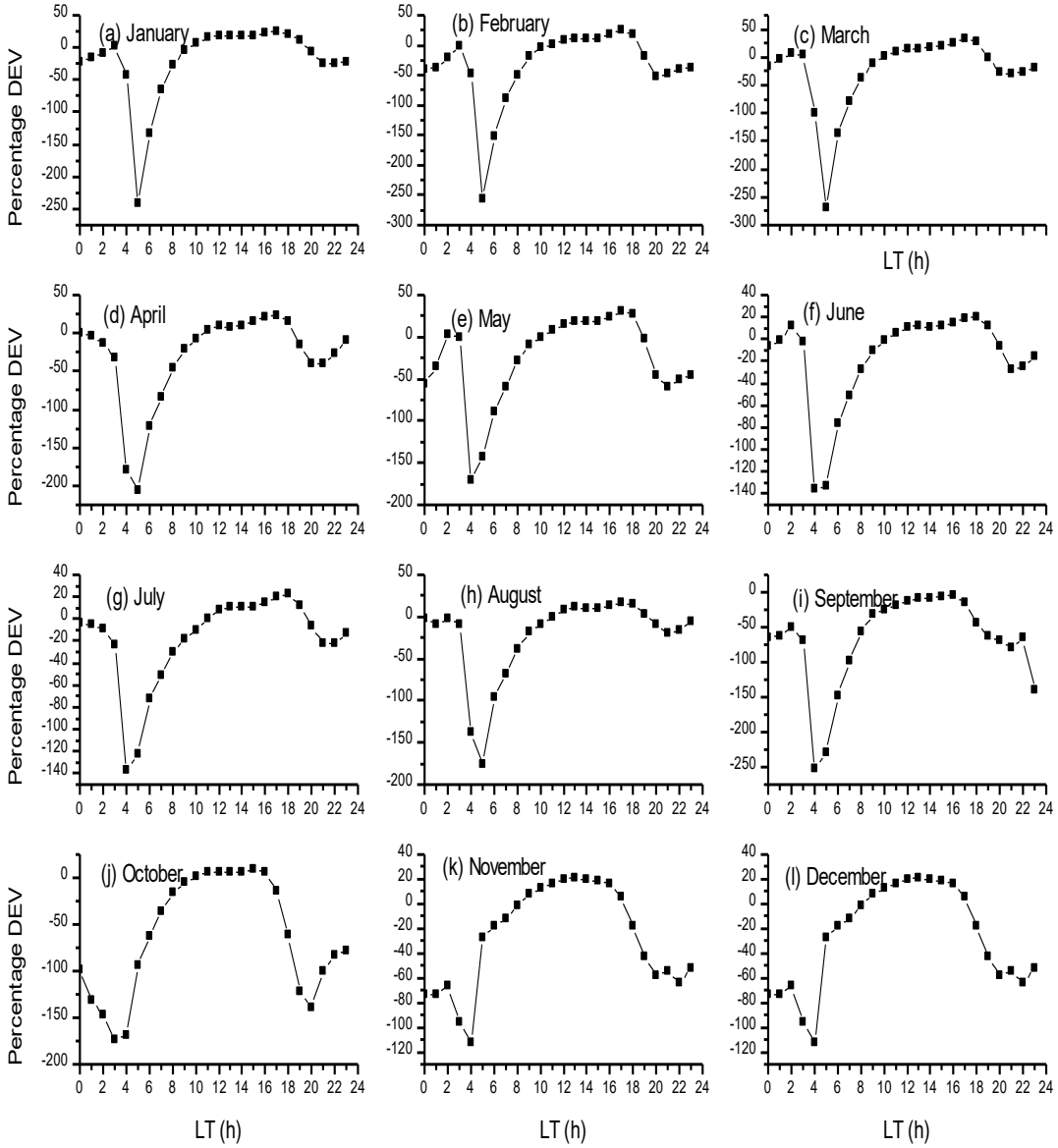

Figure 7: Percentage deviation of IRI-2016 from OBS-TEC for year 2013

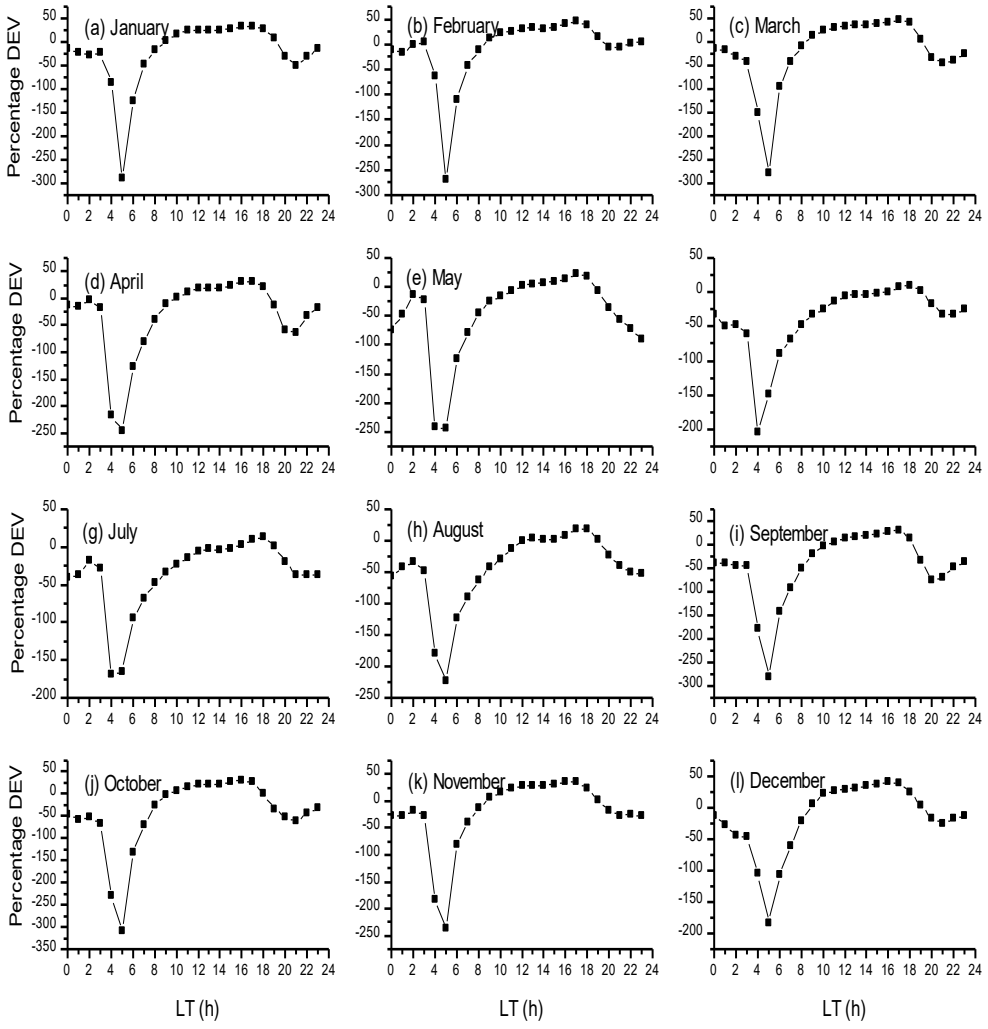

Figure 8: Percentage deviation of IRI-2016 from OBS-TEC for year 2014

The mass plots in the Figures 5 - 8 further reveal that negative percentage deviation shows higher values of IRI-2016 than OBS-TEC values. The reverse is the case for positive percentage deviation. Highest negative percentage deviations are seen between 04 – 05 LT for all months throughout the years in this study. Highest Negative percentage deviation of ~ 300% was recorded in the month of October, 2014 at 05 LT. Table II shows the summary of months with daytime over- or under-estimate of IRI-2016 in the NEI.

Table II: Months of daytime estimate of IRI-2016 model in NEI [Source: Author]

YEAR	OVER ESTIMATE	UNDER ESTIMATE	SAME RANGE
2011	January, July, August	February – April, September - December	May - June
2012		January - December	
2013	September	January – August, October - December	
2014		January - December	

Therefore, it is clear from the Figures 1- 4, Figures 5 – 8 and Table II that IRI-2016 model did not predict well in the NEI. This may be attributed to insufficient data which is as a result of the sparse distribution of GPS infrastructure in this region.

Figure 9 show plots the seasonal variations of OBS-TEC for the four years under investigation. The change in concentration of Oxygen and molecular Nitrogen has been reported to be the main cause of seasonal variation of ionospheric parameters. Seasonal variation of OBS-TEC in this study depicts semi-annual variation with equinoctial maximum (~ 52 TECU) and solsticial minimum (~ 44 TECU) in 2012. D'ujanga *et al.,* (2017) reported that since the sun passes through the equator during the equinox, both March and September equinox experience the same solar radiation. It is also a well-established fact that March 20 and September 23 are the only times in the year when the solar terminator is perpendicular to the equator, giving rise to the equinoctial maximum. The semi-annual variation resulting from the effect of equatorial ionization anomaly (EIA) in the ionosphere has been attributed to the effect of solar zenith angle and magnetic field geometry (Wu *et al.*, 2008; Rama Rao *et al.,* 2006a). Another important feature of ionospheric

parameters (known as equinoctial asymmetry) which is reported in the work of Bolaji *et al.*, (2012); Akala *et al.*, (2013); Eyelade *et al.*, (2017); D'ujanga *et al.*, (2017); Aggarwal *et al.*, (2017), is clearly seen in all years used in this work. Akala *et al.*, (2013) also reported minimum and maximum seasonal VTEC values during December solstice and June solstice respectively, during ascending phase of solar cycle 24. Equinoctial asymmetry is a strong phenomenon in low latitudes (Aggarwal *et al.*, 2017*)*. The equinoctial asymmetry has been explained in terms of the differences in the meridional winds leading to changes in the neutral gas composition during the equinoxes.

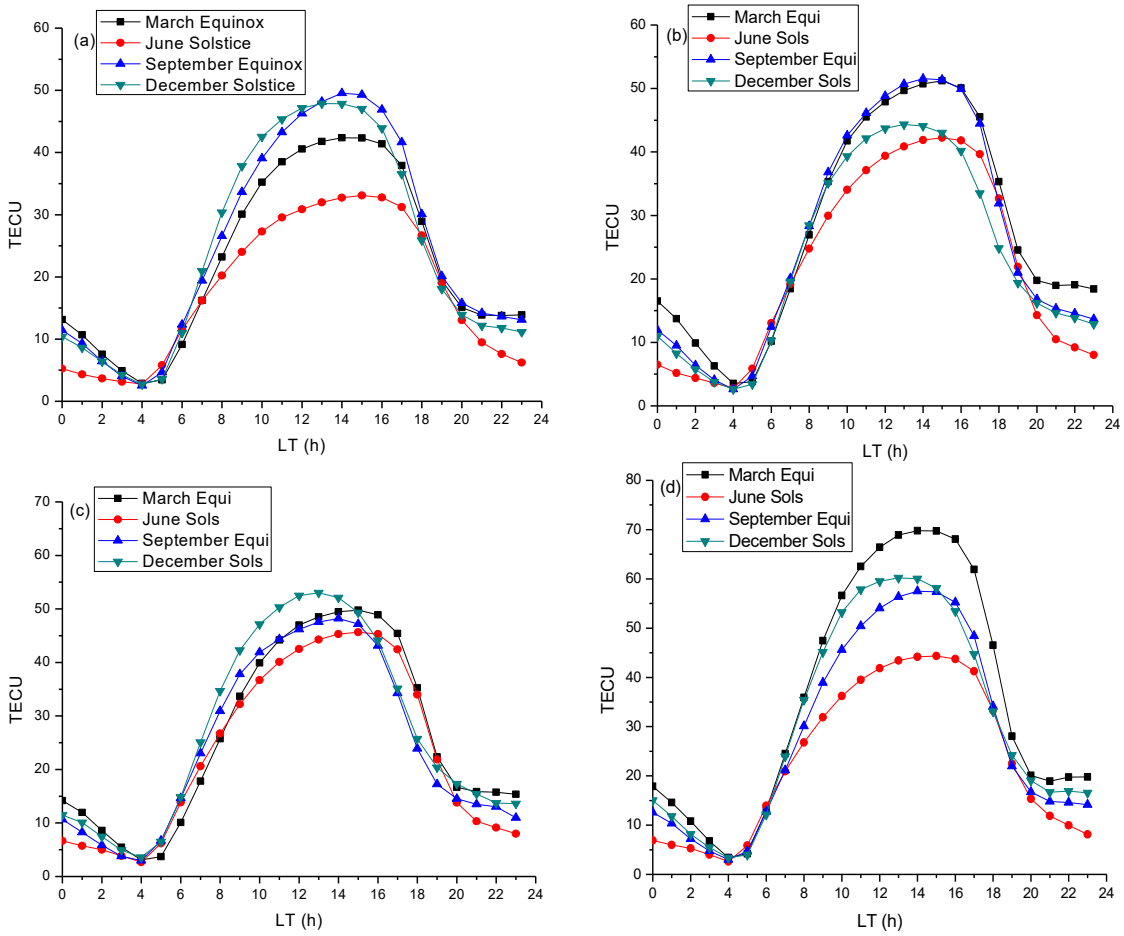

Figure 9: Seasonal variation of observed OBS-TEC during (a) 2011 (b) 2012 (c) 2013 and (d) 2014

In 2011 and 2014, the seasonal variation of OBS-TEC in the ionosphere did not follow the pattern reported by these researchers. In 2011, September equinox and December solstice recorded higher magnitude, followed by March equinox; the lowest was in June solstice. In 2013, December solstice magnitude was highest, followed by the equinoxes, March and September respectively and lowest in June solstice. This corresponds to result obtained by Akala *et al.* (2013), which they attributed to increase in ion production rate in winter season and anti-correlation between December and June Solstice pre-reversal velocity enhancement. In 2014, March equinox and December solstice magnitudes were higher than September equinox and June solstice magnitudes. December solstice magnitude is found to occur between the magnitudes of the equinoxes in 2011 and 2014. The September equinox magnitude and March equinox magnitude are observed to interchange in 2011 and 2014. Overall, June solstice magnitudes were lowest during all the years. This is due to low ionization resulting from reduced production rates, i.e. O/N_2 ratio (Titheridge 1974). Also, for all seasons, pre-midnight (18 – 23 LT) values of TEC are higher than post-midnight (00 – 05 LT) TEC values for all years. In 2011, pre- midnight TEC values are in the range of 8 – 30 TECU while post-midnight TEC values ranges from 3 to 13 TECU. In 2012, pre-midnight TEC values are in the range of 9 – 35 TECU while post-midnight TEC values are between 3 to 17 TECU. In 2013, the pre-midnight TEC values are between 9 – 35 TECU while post-midnight TEC values ranges from 3 – 15 TECU. Finally in 2014, pre-midnight TEC values are between 9 to 47 TECU while the post-midnight TEC ranges from 3 to 18 TECU.

Furthermore, the maximum OBS-TEC values in 2011 (49 TECU) and 2012 (52 TECU) were recorded in September Equinox season. In 2013, OBS-TEC reached a maximum of 53 TECU in December solstice while in 2014, the maximum OBS-TEC (70 TECU) was recorded in March

Equinox season. The corresponding annual range error (meters) of the maximum OBS-TEC using 1 TECU = 0.16m for all years are summarized in Tables III below.

Table III: Maximum OBS-TEC values and their corresponding annual range error.

YEAR	SEASON OF MAXIMUM OBS-TEC	VALUE (TECU)	CORRESPONDING ERROR (m)
2011	September Equinox	49	8
2012	September Equinox	52	8
2013	December Solstice	53	8
2014	March Equinox	70	11

Figure 10 shows the plot of annual variation of OBS-TEC and sunspot number, Rz against the months of the year from 2011 - 2014. The plots reveal the strong dependence of OBS-TEC on solar activity (sunspot number). Moreover, the ionospheric climatology especially solar activity and the equatorial ionization anomaly (EIA) effects of the ionosphere provides an insight into space weather events (Liu *et al.,* 2011). Figure 10 further reveals that TEC and sunspot number gradually increased from 2011 to 2014 of the solar cycle 24. The maximum peak of solar cycle 24 is observed in the year 2014. The sun erupted with some few major solar flares of various classes in February and October of 2014 (Kane, 2002). Hence, February, March, October and November of 2014 were months of highest TEC values. Also, an X-class type solar flare was reported in February 15, 2011. It is known fact that the increase in the sun's activities increases the electron population controlled by photoionization and recombination processes along the line of sight (LOS) from a satellite to receiver on ground.

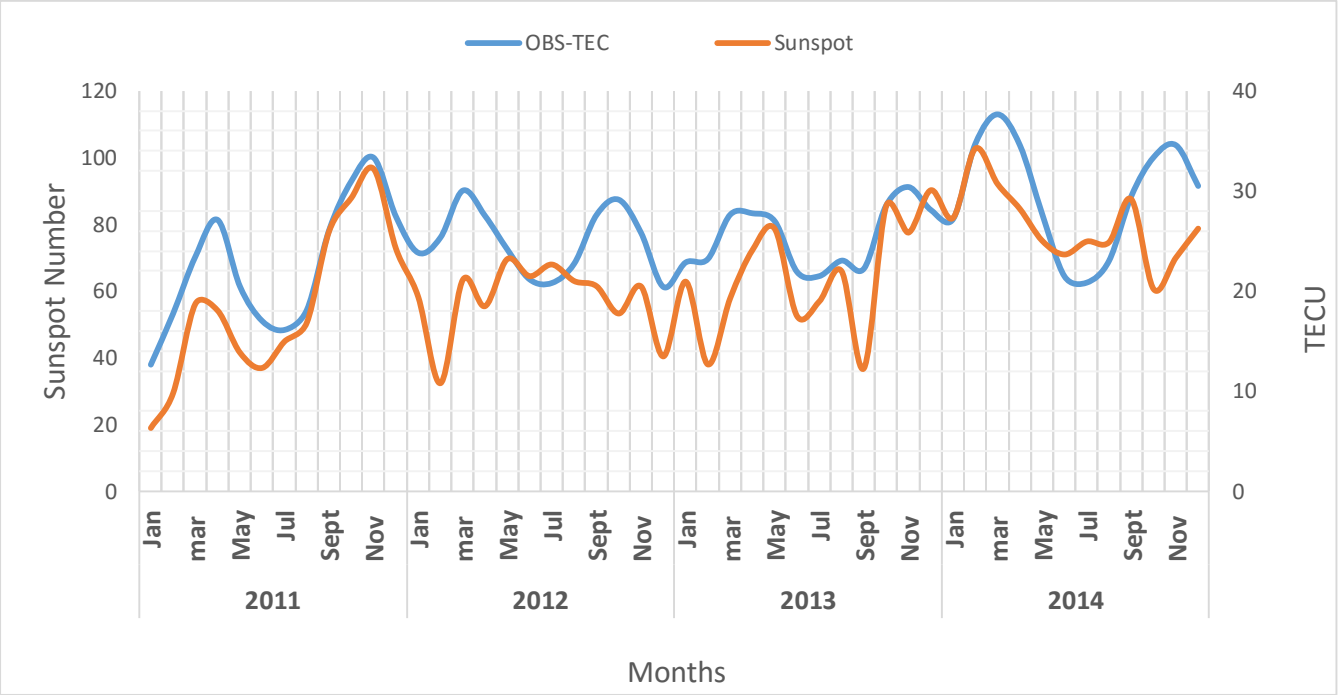

Figure 10: Annual variation of OBS-TEC and sunspot number, Rz

The effect of High solar activity in the ionosphere is solar flare of various classes, for example the $X_{2.2}$-class solar flare which occurred in February 15, 2011 (NASA, 2011). These solar flares produces waves of ionization that distorts the propagation of radio signals. When solar flare eruption becomes prominent, it flashes the earth with X- and UV radiations causing Corona Mass Ejection (CME) in the earth's direction (Kane, 2002). The shock wave travelling mass causes geomagnetic storm which may disrupt the earth's magnetosphere. CME alongside with solar flares of other origin can disrupt radio transmission, cause damage to satellites and also damage electrical transmission line facilities, resulting to long lasting power outage (National Research Council, 2008).

CONCLUSIONS

Studies on OBS-TEC and IRI-2016 model at Birnin-Kebbi in Northern Nigeria during the ascending and maximum phases of solar cycle 24 have been carried out. The result obtained reveals the following:

1. Day-to-day variations of TEC were observed to be higher during the daytime than nighttime for all the years. During the day, the sun causes variations in temperature, neutral wind, electron density and electric field in the ionosphere. The diurnal variation shows a steep rise in OBS-TEC from a minimum of ~2 TECU between 03:00 – 05:00 LT in 2011, ~3 TECU (04:00 – 05 LT) in 2012, ~3 TECU (03:00 – 05:00 LT) in 2013 and 2014. OBS-TEC increased to a broad daytime maximum between 00:12 LT – 00:14 LT for all years before falling to a minimum after sunset. The diurnal variation of IRI-2016 model shows TEC rising from a minimum of ~ 2 TECU in 2011, ~ 4 TECU in 2012 and 2013, and ~ 5 TECU in 2014 between 03:00 – 04:00hr, to a broad daytime peak between 08:00 – 14:00 LT, before falling to a minimum before sunset.
2. The diurnal variation reveals that the peak of OBS-TEC of some months were delayed till after-noon. Post-sunset decrease and enhancement due to pre-reversal zonal electric field after sunset, were also observed in the diurnal variation of OBS-TEC in some months.
3. On a general note, it can be concluded that IRI-2016 model and OBS-TEC show some discrepancies throughout the day except during the post-midnight hours (00 – 05 LT) in the NEI.
4. For all seasons, pre-midnight (18 – 23h) values of TEC are higher than post-midnight (00 – 05h) TEC values during all years. In 2011, pre- midnight TEC values are in the range of 8 – 30 TECU while post-midnight TEC values ranges from 3 to 13 TECU. In 2012, pre-midnight TEC values are in the range of 9 – 35 TECU while post-midnight TEC values are

between 3 to 17 TECU. In 2013, the pre-midnight TEC values are between 9 – 35 TECU while post-midnight TEC values ranges from 3 – 15 TECU. Finally in 2014, pre-midnight TEC values are between 9 to 47 TECU while the post-midnight TEC ranges from 3 to 18 TECU.

5. Maximum OBS-TEC values in 2011 (49 TECU) and 2012 (52 TECU) were recorded in September Equinox season. In 2013, OBS-TEC reached a maximum of 53 TECU in December solstice while in 2014, the maximum OBS-TEC (70 TECU) was recorded in March Equinox season.
6. Finally, annual variation of OBS-TEC and sunspot number, Rz against the months of the year for the four years were plotted. The plots reveal the strong dependence of TEC on solar activity (sunspot number). Solar activity and the equatorial ionization anomaly (EIA) effects of the ionosphere provides an insight into space weather events. OBS-TEC and sunspot number were found to increase gradually from 2011 to 2014.

ACKNOWLEDGEMENT

We thank the Office of the Surveyor General of the Federation (OSGoF) for making TEC data available through the infrastructure www.nignet.net. We also thank Hatanaka, Y., Gopi Krishna for providing TEC processing software online. Finally, we appreciate Bilitza e*t al.* (2017) for making the latest version of IRI model available online.

REFERENCES

Aggarwal, M., Bardhan, A., Sharma, D.K. Equinoctial asymmetry in ionosphere over Indian region during 2006 – 2013 using COSMIC measurements. Advances in Space Res., 60, 999 – 1014, 2017.

Akala, A.O., Somoye, E.O, Adeloye, A.B., Rabiu, A.B. Ionospheric f_oF_2 variability at equatorial and low latitudes during high, moderate and low solar activity. Indian Journal of Radio and Space Physics.Vol. 40, pp 124 – 129, 2011.

Akala, A.O., Seemala, G.K., Doherty, P.H., Valladares, C.E., Carrano, C.S., Espinoza, J., and Oluyo, K.S. Comparison of equatorial GPS-TEC observations over an African station and an American station during the minimum and ascending phases of solar cycle 24. Ann. Geophys., 31, 2085, 2013.

Alizadeh, M.M., Wijaya, D.D., Hobiger, T., Weber, R., Schuh, H. Ionospheric effects on microwave signals in J. Bohm and H. Schuh (eds). Atmospheric Effect in Space Geodesy. Springer atmospheric sciences. Doi: 10.1007/978-3-642-36932-2_2, © Springer-Verlag Berlin Heidelberg, 2013.

Ayorinde, T.T., Rabiu, A.B., and Amory-Mazaudier, C. Inter-hourly variability of Total Electron Content during the quiet condition over Nigeria within the Equatorial Ionization Anomaly region. J. Atmos. Solar Terr. Phys., 145, 21 – 33, 2016.

Bagiya, M.S., Joshi, H.P., Iyer, K.N., Aggarwal, M., Ravin-dran, S., and Pathan, B.M. TEC variations during low solar activity period (2005 – 2007) near the Equatorial Ionization Anomaly Crest region in India. Ann Geophys., 27, 1047 – 1057, 2009.

Bhuyan, P.K. and Borah, R.R. TEC derived from GPS network in India and comparison with the IRI. Advances in Space Res., 39, 830 – 840, 2007.

426 Bilitza, D., Altadill, D., Zhang, Y., Mertens, C., Truhlik, V., Richards, P., McKinnell, L.A.,
427 Reinisch, B. International reference ionosphere 2012 – A model of international collaboration. J.
428 Space Weather Space Clim., 4, 1 – 12, doi: 10.1002/201JA018009, 2014.

429 Bilitza, D., Altadill, D., Truhlik, V., Shubin, V., Galkin, I., Reinisch, B., and Huang, X.
430 International reference ionosphere 2016: from ionospheric climate to real-time weather
431 predictions. Space weather, 15, 418 – 429, doi: 10.1002/20165SW001593, 2016.

432 Bolaji, O. S., Adeniyi, J.O., Radicella, S.M., and Doherty, P.H. Variability of total electron content
433 over an equatorial West African station during low solar activity. Radio Sci., 47, RS1001, doi:
434 10.1029/2011RS004812, 2012.

435 Ciraolo, L., and Spalla, P. TEC analysis of IRI simulated data. Adv. Space Res., 29, 6, 959 – 966,
436 2002.

437 Codrescu, M. V., Palo, S. E., Zhang, X., Fuller-Rowell, T. J., Poppe, C. TEC climatology derived
438 from TOPEX/POSEIDON measurements, Journal of Atmospheric Solution, 61, 281-298, 1999.

439 Dabas, R.S., Singh, L., Lakshmi, D.R., Subramanyam, P., Chopra, P., Garg, S.C. Evolution and
440 dynamics of equatorial plasma bubbles: relationships to **E** × **B** drifts, post-sunset total electron
441 content enhancements, and equatorial electrojet strength. Radio Sci., 38, doi:
442 10.1029/2001RS002586, 2003.

443 D'ujanga, F.M., Opio, P. Twinomugisha, F. Variation of total electron content with solar activity
444 during the ascending phase of solar cycle 24 observed at Makerere University, Kampala. Space
445 Weather: Longitude and Hemispheric Dependences and Lower Atmosphere Forcing, Geophysical
446 Monograph 220, First Edition. Edited by Timothy Fuller-Rowell, Endawoke Yizengaw, Patricia

H. Doherty, and Sunanda Basu. © 2017 American Geophysical Union. Published 2017 by John Wiley & Sons, Inc., 2017.

Eyelade, V.A., Adewale, A.O., Akala, A.O., Bolaji, O.S. and Rabiu, A.B. Studying the variability in the diurnal and seasonal variations in GPS TEC over Nigeria. Ann. Geophys., 35, 701 – 710, 2017.

Fayose, R.S., Rabiu, B., Oladosu, O., Groves, K. Variation of total electron content (TEC) and their effect on GNSS over Akure. Nigeria, Applied Physics Research, 4, 2, 2012.

Forbes, J.M., Bruinsma, S., Lemoine, F.G. Solar rotation effects in the thermospheres of Mars and Earth. Science, 312, 1366–1368, 2006.

Gorney, D. J. Solar cycle effects on the near-earth space environment. Rev Geophys, 28, 315–336, 1990.

Hajra, R., Chakraborty, S.K., Tsurutani, B.T., DasGupta, A., Echer, E., Brum, C.G.M., Gonzalez, W.D., Sobral, H.A. An empirical model of ionospheric total electron content (TEC) near the crest of the equatorial ionization anomaly (EIA). J. Space Weather Space Clim., 6, A29, doi: 10.1051/swsc/2016023, 2016.

Liu, L., Wang, W., Chen, Y., Le, H. solar activity effects on the ionosphere: A brief review. Space Physics and Space Weather Geophysics. Chinese science Bulletin. 56, 12, 1202 – 1211, 2011.

Jee, G., Schunk, R. W., Scherliess, L. Analysis of TEC data from the TOPEX/Poseidon mission, Journal of Geophysical Research, 109, A01301, doi:10.1029/2003JA010058, 2004.

Kane, R.P. Some implications using the group sunspot number reconstruction. Solar Phys., 205, 2, 383 – 401, 2002.

468 Komjathy, A., Langley, R., Bilitza, D. ingesting GPS-derived data into the IRI for single frequency
469 radar altimeter ionospheric delay corrections. Adv. Space Res., 22, 6, 793 – 802, 1998.

470 Langley, R., Fedrizzi, M., Paula, E., Santos, M., Komjathy, A. Mapping the low latitude
471 ionosphere with GPS. GPS World, 13, 2, 41 – 46, 2002.

472 Lee, C.C. and Reinisch, B.W. Quiet condition hmF2, NmF2 and Bo variations at Jicamarca and
473 comparison with IRI-2001 during solar maximum. J. Atmos. Solar Terr. Phys., 68, 2138 – 2146,
474 2006.

475 Maruyama, T., Ma, G., and Nakamura, M. Signature of TEC storm on 6 November 2001 derived
476 from dense GPS receiver network and ionosonde chain over Japan. Journal of Geophysical
477 Research, 109, A10302, doi:10.1029/2004JA010451, 2004.

478 National Research Council. Space Weather Events: Understanding Societal and Economic impact:
479 A workshop Report, Washington DC: National Academia Press, p-177. ISBN: 978-0-039-12769-
480 1, 2008.

481 NASA. (2011). Valentine's Day Solar Flare, NASA, February 17, 2011. Retrieved Semptember
482 09, 2014, from http://www.nasa.gov/mission_pages/sunearth/news/ News021411-xclass.html, last
483 accessed October 29, 2014.

484 Okoh, D., Lee-Anne McKinnell, L., Cilliers, P., Okere, B., Okonkwo, C., Rabiu, A.B. IRI-VTEC
485 versus GPS-vTEC for Nigerian SCINDA GPS stations. Advances in Space Research,
486 http://dx.doi.org/10.1016/j.asr.2014.06.037, 2014.

487 Ogunmodimu, O., Rogers, N.C., Falayi, E., Bolaji, S. Solar Flare induced cosmic noise absorption,
488 NRIAG Journal of Astronomy and Geophysics. 7, 1, 31-39, 2018.

Ogwala, A., Somoye, E.O., Oyedokun, O., Adeniji-Adele, R.A., Onori, E.O., Ogungbe, A.S., Ogabi, C.O., Adejo, O., Oluyo, K.S., Sode, A.T. Analyses of Total Electron Content over Northern and Southern Nigeria. J. Res. and Review in Sci., 21 – 27, 2018.

Onwumechilli, C.A., and Ogbuehi, P.O. Journal Atmos. Terr. Phys., 26, 894, 1964.

Rama Rao, P.V.S., Krishna, S.G., Prasad, J.V., Prasad, S.N.V.S., Prasad, D.S.V.V.D., Niranjan, K. Geomagnetic storm effects on GPS based navigation. Ann. Geophys., 27, 2101 – 2110, 2009.

Rama Rao, P.V.S., Krishna, S.G.,Niranjan, K., Prasad, D.S.V.V.D. Study of temporal and spatial characteristics of L-band scintillation over the Indian low-latitude region and their possible effects on GPS navigation. Ann. Geophys., 24, 1567 – 1580, 2006a.

Rama Rao, P.V.S., Krishna, S.G.,Niranjan, K., Prasad, D.S.V.V.D. Temporal and spatial variations in TEC using simultaneous measurements from indian GPS network of receivers during low solar activity period of 2004 – 2005. Ann. Geophys., 24, 3279 – 3292, 2006b.

Rama Rao, P.V.S., Niranjan, K., Prasad, D.S.V.V.D., Krishna, S.G., Uma, G. On the validity of the ionospheric pierce point (IPP) altitude of 350km in the Indian equatorial and low-latitude sector. Ann. Geophys., 24, 2159 – 2168, 2006c.

Suranya, P.L., Prasad, D.S.V.V.D., Niranjan, K., Rama Rao, P.S.V. Short term variability in foF2 and TEC over low latitude stations in the Indian sector. Indian J. of Radio and Space Phys., 44, 14 – 27, 2015.

Somoye, E.O. Diurnal and seasonal variation of fading rates of E- and F-region echoes during IGY and IQSY at the equatorial station of Ibadan. Indian Journal of Radio and space Physics, 38, 194 – 202, 2010.

510 Somoye, E.O., Akala, A.O., Ogwala, A. Day-to-day variability of h'F and foF2 during some solar
511 cycle epochs. Journal Atmos. Solar Terr. Physics, 73, 1915 – 1922, 2011.

512 Stankov, S. M. Trans-ionospheric GPS signal delay gradients observed over mid-latitude Europe.
513 Advances in Space Research, 43, 1314–1324, 2009.

514 Tariku, Y.A. Pattern of GPS-TEC variability over low-latitude regions (African sector) during the
515 deep solar minimum (2008 to 2009) and solar maximum (2012 to 2013) phases. Earth, Planets,
516 and space. 67, 35, 2015.

517 Titheridge, J.E. Changes in atmospheric composition inferred from ionospheric production rates.
518 J. Atmos. Terr. Phys., 36, 1249 – 1257, 1974.

519 Wanninger, L. Effects of the equatorial ionosphere on GPS. GPS World, 2, 48, 1993.

520 Wu, C.C., Liou, K., Shan, S.J., Tseng, C.L. Variation of ionospheric total electron content in
521 Taiwan region of the equatorial anomaly from 1994 – 2003. Adv. Space Res., 41, 611 – 616, 2008.

522

523